

## BINARY COLLISION MONTE CARLO SIMULATIONS OF CASCADES IN POLYATOMIC CERAMICS \*

N.M. GHONIEM and S.P. CHOU

*University of California, Los Angeles, Los Angeles, CA 90024, USA*

The understanding of radiation damage phenomena in polyatomic ceramic materials (PCMs) is still at an early stage as compared to that in metallic structural alloys. The binary collision approximation (BCA) is used in a Monte Carlo (MC) study of high-energy collision-cascade creation in SPINEL ( $\text{MgAl}_2\text{O}_4$ ). The study focuses on two aspects of cascade generation: cascade morphology and cascade stoichiometry. In the high-energy regime, typical of fusion neutrons, cascades show a tree-like morphology. To a large degree, instantaneous recombination occurs in the “stem” part of the cascade because of the closer separation of vacancy–interstitial pairs. Following this recombination phase, fusion neutron cascades tend to result in Frenkel pairs distributed on the “branches” of the tree in a zone extending over 100 to 200 nm. The stoichiometry of displacements within the cascade is found to be substantially different from bulk stoichiometry, and is dependent upon the energy and type of primary knock-on atom (PKA). Limitations of the BCA to model the low energy characteristics of the cascade are discussed in the paper.

### 1. Introduction

Polyatomic ceramic insulators are proposed for a variety of applications in fusion reactors (e.g., waveguides and dielectric windows). They must be used to insulate between conductor turns in normal magnet designs. In some designs, such as the reversed field pinch (RFP) concept [1], insulating materials are used as part of the design of the conducting shell (or first wall), and also in the breeding blanket of the system. The use in this case stems from the need to reduce toroidally continuous eddy currents that are detrimental to plasma stability. The magnetohydrodynamic (MHD) force opposing liquid–metal fluid flow in self-cooled liquid-metal blankets is by far the most serious design problem in these types of blankets. Without insulated walls, the MHD force can be more than an order of magnitude larger than the same design with wall insulation [1]. Ceramic insulators are therefore proposed in applications ranging from low neutron flux/low temperature conditions to locations near the first wall where both the neutron flux and temperature are high.

Spinel,  $\text{MgAl}_2\text{O}_4$ , appears to be a primary candidate for these applications. Irradiation to  $2 \times 10^{26}$  n/m<sup>2</sup> at 1100 K produced no void swelling of single-crystal  $\text{MgAl}_2\text{O}_4$  [2]. Low swelling rates of spinel have also been observed by a number of investigators [3,4]. The strength of spinel has been observed to be enhanced by neutron irradiation [3]. The lack of significant swelling under irradiation has been attributed to the nature of generation, recombination, and agglomeration of defects [5]. In particular, the lack of helium bubble nuclei and the absence of dislocation loops which are precursors to swelling were proposed as reasons for swelling resistance. In an experimental study by Buckley [6], 1-MeV electron irradiation of spinel samples preim-

planted with 1000 ppm helium atoms resulted in no observable loops or voids after 10 to 30 dpa. Coghlan et al. [7] presented results of swelling saturation for relatively low neutron fluences ( $\approx 2 \times 10^{22}$  n/m<sup>2</sup>,  $E > 0.1$  MeV) at 50 °C. They attributed the swelling saturation to interstitial-type defects leading to point–defect recombination and swelling saturation.

To understand the nature of displacement damage in spinel, the primary damage state must be carefully analyzed. The complex crystal structure of the material renders simple extrapolations from metallic alloys unreliable. Using a continuous slowing-down theory of collision cascades, Parkin and Coulter [8–10] showed that the structure of cascades in polyatomic materials is quite complex, and that cascade stoichiometry generally differs from that of the bulk material. Itoh and Tanimura [11] indicated that in addition to the production of Frenkel pairs by the atomic displacement process, stable point defects can be produced from self-trapped excitons in certain materials.

In a fusion neutron environment, PKAs may be initiated with kinetic energies of several MeV. A molecular dynamics (MD) simulation of cascades generated by such high energy PKAs is still not achievable. On the other hand, analytical approximations of cascade behavior may not accurately represent important details. In this paper, we present results of cascade simulations using the BCA, and we illustrate the nature of the primary damage generation by a study of cascade morphology and stoichiometry in spinel.

### 2. Monte Carlo model

The Monte Carlo transport code, TRIPOS, (transport of ions in polyatomic multi-layer solids) has been developed for the analysis of bulk and surface primary damage [12,13]. The code is based on the binary collision approximation for an amorphous solid. The free path between collisions, and the nuclear energy transfer

\* Work supported by the US Department of Energy, Office of Fusion Energy, Grant #DE-FG03-84ER52110, with UCLA.

and scattering angle are accurately calculated by using the power-law cross sections and a new method for general interatomic potentials [14].

The free path between collisions is estimated from the probability of interaction using the total scattering cross section. In the BCA, a moving atom can interact with only one medium atom at a time. The total interaction cross section is first calculated as a linear stoichiometric sum of individual atomic cross sections. The type of recoil is determined randomly from the ratio of an atomic cross section to the total cross section. The mass and energy dependence of cross sections dictate, therefore, the stoichiometry of recoils within the cascade.

Recoils travel between these discrete collisions losing part of their energy continuously to electrons. In one version of the code, TRIPOS-E [15], energy transfers to electrons are discretely treated and distributions of electron-hole (e-h) pairs along ion tracks are calculated. Nevertheless, we do not include here the effects of exciton relaxation on stable Frenkel-pair generation as proposed by Itoh and Tanimura [11]. Approximately 10 keV of electronic energy deposition is required for the production of a Frenkel pair through this mechanism, which indicates that the contributions of these events to total displacements are negligible in a fusion environment. Therefore, the results presented here are limited by the validity of the BCA, and no attempt is made to include mechanisms of low energy dissipation. The basic problem we confront is that the size of a fusion collision cascade results in computational irreducibility if a direct MD approach is used, particularly when electronic excitational energy transfers are simulated. The BCA is deemed to give a reasonable description of the general features of collision cascades. The contributions of low-energy correlated-collision sequences were observed in several MD calculations [16,17]. However, Hou and Todorov [18] noted the similarity of cascade simulation results between BCA and MD approaches.

The value of the minimum displacement threshold,  $E_d$ , of individual atoms in a polyatomic material has an important influence on cascade properties. This value is difficult to measure, and a wide range is reported in the literature. Crawford [19] used the values of 86 eV for Mg, 77 eV for Al, and 130 eV for O. Summers et al. [20] reported a value of 59 eV for O, while Matzke [21] used a similar value of 56 eV for O. Itoh and Tanimura [11] indicated that  $E_d$  for Al and Mg is in the range 18 to 30 eV. In view of these uncertainties, we show the effects of displacement threshold energy by studying two illustrative conditions.

### 3. Discussion of results

Near the first wall of a fusion reactor, the majority of neutrons will have energies in the range of 14 MeV. These neutrons generate PKAs with average energy on the order of several MeV. Fig. 1 shows a three-dimen-

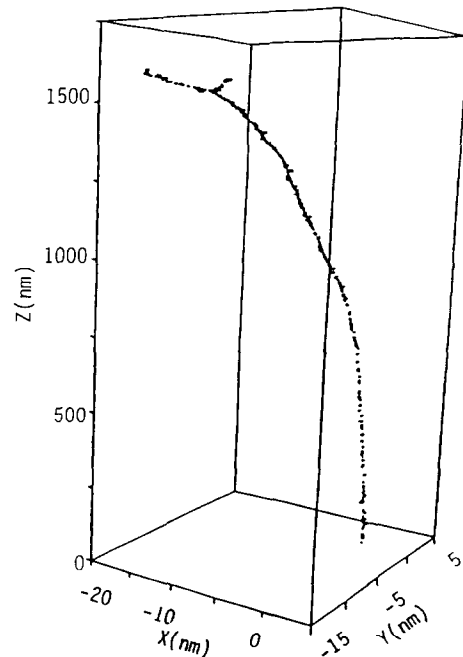


Fig. 1. Fusion neutron cascade simulation (3-D) in spinel (PKA = 0.2 MeV energy).

sional (3-D) simulation of anion and cation interstitials, before instantaneous recombination, in a collision cascade initiated by a 2 MeV oxygen PKA. The cascade exhibits a tree-like morphology, with a relatively long “stem” and self-similar “branches” towards the top. When instantaneous recombination is allowed with a recombination radius of 1.0 nm, the stem portion undergoes more complete recombination events than the branches (fig. 2). Coulombic energy transfers tend to favor recoils with small energies, thus resulting in point defects at close separation. As the PKA slows down, large-angle collisions occur with higher probabilities and point defects are produced at larger separations.

Cascade stoichiometry is described by the chemical composition of a molecular displacement. At the end of the cascade propagation phase, the cascade is said to be stoichiometric if atoms are displaced at the ratios 1 : 2 : 4 for Mg, Al, and O, respectively. A nonstoichiometric cascade is represented by the formula  $MgAl_{2+x}O_{4+y}$ , where  $x$  is the excess aluminum displacements and  $y$  is the excess oxygen displacements, as normalized to Mg displacements. The first set of calculations are performed for equal  $E_d$ ; 56 eV for Al, Mg, and O. Fig. 3 shows the dependence of the excess stoichiometry,  $x$ , on the PKA energy, where cascades are initiated with O, Mg, or Al PKAs. At high PKA energies, cascade mixing eliminates the dependence of  $y$  on the PKA type. At lower energies, however, PKAs distribute their energy preferentially to the corresponding lattice atoms. This  $x$  is positive for Al PKA and negative for both O and Mg

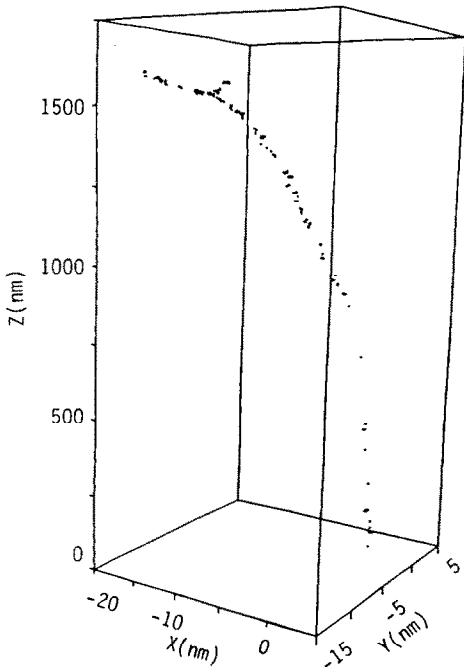


Fig. 2. Cascade simulation (3-D) in spinel allowing for instantaneous recombination (PKA = 0.2 MeV energy).

PKAs. It is to be noted here that even with a species-independent displacement threshold, differences in mass and charge appear in the interaction cross sections. Energy partitioning favors displacement of higher mass atoms.

Fig. 4 shows the total number of displacements per PKA as a function of the PKA energy. The solid lines with heavy dots result from analytical calculations based on Lindhard's theory for comparison [22]. The displacement threshold is taken as 56 eV for the three elements. It is interesting to note that over a wide range of PKA energies, the number of displacements per PKA is independent of the PKA type. This behavior extends up to

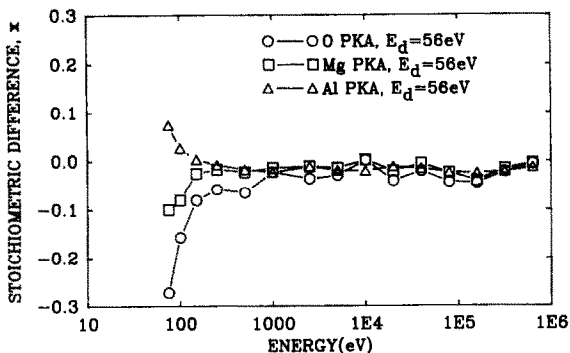


Fig. 3. Aluminum stoichiometric excess ( $x$ ) in spinel as a function of various PKA energies.

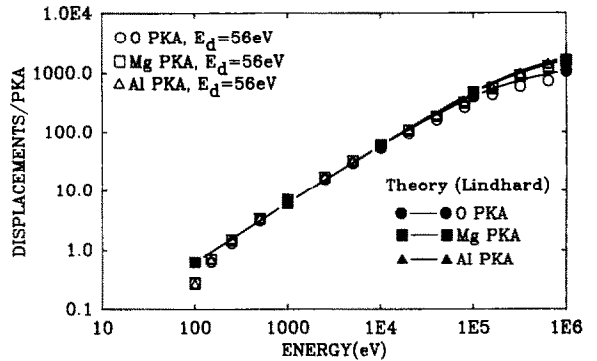


Fig. 4. Comparison between TRIPOS results and Lindhard's theory for the total number of displacements per PKA.

PKA energies in the range of  $\sim 30$  to 100 keV. Above this range, electronic energy loss is PKA dependent. Larger PKA masses tend to produce more displacements, as is well known from simple analytical cascade theories.

The next set of calculations are performed for displacement threshold energies that are energy dependent.  $E_d$  is taken as 56 eV for oxygen, and it is assumed to be 18 eV for both Al and Mg. Fig. 5 shows the stoichiometric excess (or deficiency),  $y$ , as a function of the PKA energy. The higher oxygen displacement threshold results in a dramatic decrease in  $y$  over the entire PKA energy range. In the lower range of PKA energies, a significant fraction of recoils is generated with energies close to the oxygen displacement threshold. Cascades propagate entirely on the cation sublattice, when PKAs are initiated with a few hundred eV.

Since the mass difference between Al and Mg is not very large, and since they both have the same displacement threshold, the magnitude of  $x$  is much smaller than  $y$ . Our calculations indicate that the dependence on PKA type is not significant, particularly at high PKA energies. In the low energy regime, however, a

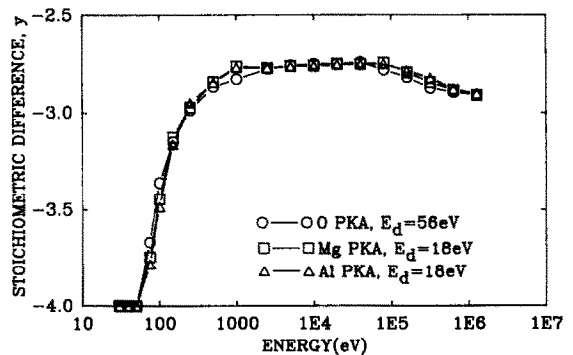


Fig. 5. Oxygen stoichiometric excess ( $y$ ) in spinel as a function of various PKA energies.

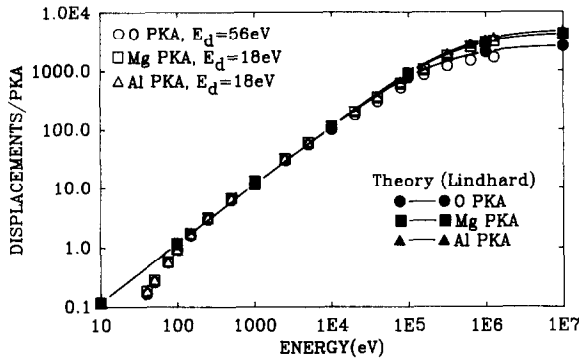


Fig. 6. Comparison between TRIPOS results and Lindhard's theory for the total number of displacements ( $E_d$  weighting is used).

slight preferential energy coupling with Mg is noticed; hence negative values of  $x$  are observed. For the same conditions, the number of displacements per PKA is shown as a function of the PKA energy in fig. 6. Calculations using Lindhard's theory with an effective displacement threshold are also shown for comparison with Monte Carlo results. The major fraction of knock-ons have low energies, close to the displacement threshold. Our analytical theory of cascade slowing down in an infinite medium indicates that the number of knock-ons  $N$  is energy dependent in the form [23]

$$N(E) \sim \frac{1}{E^{5/2}}. \quad (1)$$

Eq. (1) is based on a hard-sphere scattering cross section which usually overestimates low energy transfers. Empirically, an effective value of the displacement threshold is therefore suggested as

$$E_d^c = \left[ \sum_i S_i E_{d,i}^{-n} \right]^{-1/n}, \quad (2)$$

where  $E_d^c$  is the effective displacement threshold and  $S_i$  is the stoichiometry of the element with a displacement threshold  $E_{d,i}$ . Application of Lindhard's theory, together with eq. (2), shows good agreement with MC calculations for  $n = 1$  (fig. 6). In all MC calculations, the relative uncertainty in  $y$  is  $< 3\%$ . For  $x$ , however, the absolute uncertainty is  $< 0.005$  for high energy cases and is  $< 0.02$  for low energy cases.

#### 4. Conclusions

Displacement cascade morphology in polyatomic ionic solids in a fusion environment is similar to previous simulations of cascades in a metallic structure. The BCA shows large cascade dimensions (on the order of 100 to 200 nm). Cascades resulting from high energy neutrons show a tree-like morphology with more instantaneous recombination occurring in the stem part of

the cascade. The stoichiometry of cascades in spinel shows a large oxygen deficiency. This oxygen displacement deficiency is even more dramatic if a higher O displacement threshold is used. Cascade mixing eliminates the dependence of this deficiency on the type of PKA for high energy. Low energy PKAs tend to favor coupling with like atoms, thus introducing O displacement deficiency when Al or Mg PKAs are used for the case of equal displacement thresholds. If it is experimentally confirmed that the displacement threshold for O is higher than or Al and Mg, experimental simulation with ions, electrons, or fission neutrons may therefore be inaccurate representations of fusion neutron cascades. The total number of displacements in a ceramic can be calculated by Lindhard's theory, provided that an effective displacement threshold is used. This effective value is obtained by applying the suggested eq. (2).

It is to be noted that two areas of uncertainties still exist in the present calculations. The first uncertainty is the questionable validity of the BCA for low energy collisions. The exact locations of displaced atoms may be uncertain. The second uncertainty is cascade structure after immediate point-defect recombination and cascade cooling. As indicated earlier, this phase has been simply treated parametrically by variation of the value of the recombination radius. The overall features of high energy cascades in polyatomic ceramics are believed to be revealed by the current application of the BCA. However, more detailed information should probably be obtained by molecular dynamics.

The authors would like to acknowledge the support of the US Department of Energy, Office of Fusion Energy, Grant #DE-FG03-84ER52110, with UCLA.

#### References

- [1] F. Najmabadi et al., The Titan Reversed-Field Pinch Fusion Reactor Study, Scoping Phase Report, University of California, Los Angeles Report No. UCLA-PPG-1100 (1987).
- [2] F.W. Clinard Jr., G.F. Hurley and L.W. Hobbs, *J. Nucl. Mater.* 108 & 109 (1982) 655.
- [3] G.F. Hurley, J.C. Kennedy, F.W. Clinard Jr., R.A. Youngman and W.R. McDonell, *J. Nucl. Mater.* 103 & 104 (1981) 761.
- [4] F.W. Clinard Jr., G.F. Hurley, R.A. Youngman and L.W. Hobbs, *J. Nucl. Mater.* 133 & 134 (1985) 701.
- [5] L.W. Hobbs and F.W. Clinard, Jr., *J. Phys. (Paris)* 41 (1980) C6-232.
- [6] S.N. Buckley, *J. Nucl. Mater.* 141-143 (1986) 387.
- [7] W.A. Coghlan, F.W. Clinard, Jr., N. Itoh and L.R. Greenwood, *J. Nucl. Mater.* 141-143 (1986) 382.
- [8] D.M. Parkin and C.A. Coulter, *J. Nucl. Mater.* 101 (1981) 261.
- [9] C.A. Coulter and D.M. Parkin, *J. Nucl. Mater.* 85 & 86 (1979) 611.

- [10] D.M. Parkin and C.A. Coulter, *J. Nucl. Mater.* 103 & 104 (1981) 1315.
- [11] N. Itoh and K. Tanimura, *Radiat. Eff.* 98 (1986) 269.
- [12] P. Chou and N. Ghoniem, *J. Nucl. Mater.* 117 (1983) 55.
- [13] P. Chou and N. Ghoniem, *Nucl. Instr. and Meth. B28* (1987) 175.
- [14] J. Blanchard, P. Chou and N. Ghoniem, *J. Appl. Phys.* 61 (1987) 3120.
- [15] R.C. Martin and N.M. Ghoniem, *Phys. Status Solidi A104* (2) (1987).
- [16] J.B. Gibson, A.N. Goland, M. Milgram and G.H. Vineyard, *Phys. Rev.* 120 (1960) 1229.
- [17] C. Erginsoy, G.H. Vineyard and A. Englert, *Phys. Rev.* A133 (1965) 535.
- [18] M. Hou and S. Todorov, *Phys. Lett.* A91 (1982) 461.
- [19] J.H. Crawford, Jr., *Adv. Phys.* 17 (1968) 93.
- [20] G.P. Summers, G.S. White, K.H. Lee and J.W. Crawford, *Phys. Rev.* B21 (1980) 2575.
- [21] Hj. Matzke, *Radiat. Eff.* 64 (1982) 3.
- [22] J. Lindhard, V. Nielsen, M. Scharff and P.V. Thomsen, *K. Dan. Vidensk. Selsk., Mat. Fys. Medd.* 33, 10 (1963).
- [23] P.S. Chou and N.M. Ghoniem, *Nucl. Instr. and Meth. B9* (1985) 209.